Title

Effect of myeloperoxidase inhibition on gene expression profiles in HL-60 cells exposed to 1, 2, 4,-benzenetriol

Author names and affiliations

Emiko Miyahara[a,b], Takuro Nishikawa[a,b], Toru Takeuchi[a], Kaori Yasuda[c], Yasuhiro Okamoto[b], Yoshifumi Kawano[b], Masahisa Horiuchi[a]

[a]Department of Hygiene and Health Promotion Medicine, [b]Department of Pediatrics, Graduate School of Medical and Dental Sciences, Kagoshima University, Kagoshima, Japan

[c]Cell Innovator Inc., Venture Business Laboratory of Kyushu University, Fukuoka, Japan

Corresponding author: Takuro Nishikawa

Department of Pediatrics, Kagoshima University Graduate School of Medical and Dental Sciences, 8-35-1 Sakuragaoka, Kagoshima City, 890-8520 Japan

TEL; +81-99-275-5354, FAX; +81-99-265-7196,

E-mail; adu44150@ams.odn.ne.jp

Abstract

While it is known that benzene induces myeloid leukemia in humans, the mechanism has yet to be clarified. Previously, we suggested that myeloperoxidase (MPO) was the key enzyme because it promotes generation of powerful oxidant hypochlorous acid (HOCl) which, reacting with DNA, causes leukemogenesis. In this study, using a whole-human-genome oligonucleotide microarray to clarify the relationships between myelotoxicity of benzene and MPO, we analyzed the genome-wide expression profiles of HL-60 human promyelocytic cell lines exposed to 1,2,4-benzenetriol (BT) with or without MPO inhibition. The microarray analysis revealed that short (1 h) and longer (4 h) exposure to BT changed the expression in HL-60 cells of 1,213 or 1,214 genes associated with transcription, RNA metabolic processes, immune response, apoptosis, cell death, and biosynthetic processes ($|Z\text{-score}| > 2.0$), and that these changes were dramatically lessened by MPO-specific inhibition. The presence of functionally important genes and, specifically, genes related to apoptosis, carcinogenesis, regulation of transcription, immune responses, oxidative stress and cell-cycle regulation were further validated by real-time RT-PCR.

Gene expression profiles along with Gene Ontology (GO) and Kyoto Encyclopedia of Genes and Genomes (KEGG) pathway annotation analysis suggest that BT-induced DNA halogenation by MPO is a primary reaction in the leukemogenesis associated with benzene.

Highlights

- With MPO inhibition, BT hardly increased apoptosis in HL-60 cells.
- BT did not increase apoptosis in U937 cells, which express no MPO.
- BT changed the expression levels of many genes in HL-60 cells.
- BT mainly affected mRNA levels of genes related to apoptosis and antiapoptosis.
- MPO inhibition dramatically suppressed the effects of BT on gene expression.

Key words

1,2,4-benzenetriol, microarray, acute myeloid leukemia, myeloperoxidase, hypochlorous acid, reactive oxygen species

Abbreviations

ABAH, 4-aminobenzoic acid hydrazide; AML, acute myeloid leukemia; BT, 1,2,4-benzenetriol; BQ, 1,4-benzoquinone; Ct, cycle time; DAVID, Database for Annotation, Visualization and Integrated Discovery; DPBS, Dulbecco's phosphate-buffered saline; FBS, fetal bovine serum; FITC, fluorescein isothiocyanate; GAPDH, glyceraldehyde-3-phosphate dehydrogenase; GEO, Gene Expression Omnibus; GO, Gene Ontology**;** HCL, hierarchical clustering; H_2O_2, hydrogen peroxide; HOCl, hypochlorous acid; HQ, 1,4-hydroquinone; KEGG, Kyoto Encyclopedia of Genes and Genomes; MAPK, mitogen-activated protein kinase; MPO, myeloperoxidase; NCBI, National Center for Biotechnology Information; NLR, NOD-like receptor; $O_2^{\bullet-}$, superoxide; •OH, hydroxyl radical; PBS, phosphate buffered

saline; PI, propidium iodide; ROS, reactive oxygen species; SE, standard error; siRNA, small interfering RNA.

Introduction

Benzene is widely used in the petrochemical industry, for example, in gasoline production, and is present in cigarette smoke. It is reported to be myelotoxic, and thus liable to cause aplastic anemia and acute myeloid leukemia (AML) (Aksoy, 1989; Huff, 2007). The mechanisms underlying leukemogenesis, however, have yet to be clarified. When benzene gets into the body, it is primarily metabolized in the liver by cytochrome P450 2E1 to benzeneoxide. This benzeneoxide is subsequently converted to various metabolites (Snyder and Hedli, 1996). One of these metabolites, 1,2,4-benzenetriol (BT), with a triphenolic structure, strongly reacts with molecular oxygen. It has been reported that BT induces oxidative DNA damage and breaks DNA strands (Kawanishi et al., 1989; Kolachana et al., 1993; Lewis et al., 1988).

Myeloperoxidase (MPO), which is released from the cytoplasmic granules of neutrophils, catalyzes the formation of hypochlorous acid (HOCl), a highly reactive oxidant derived at neutral pH from hydrogen peroxide (H_2O_2) and chloride ions in physiological plasma concentrations of halide (Harrison and Schultz, 1976; Klebanoff, 1999). The major product of neutrophil MPO, HOCl is a potent cytotoxin that plays key roles in host defense responses by oxidizing the cellular constituents of invading pathogens (Hurst and Barrette, 1989). HOCl, however, is also capable of damaging host tissue such as proteins, lipids, and nucleic acids (Heller et al., 2000). MPO-induced

DNA halogenation or protein damage or both might be implicated in the association between chronic inflammation and cancer (Ward, 1987; Marnett, 2000).

In previous studies, we found that exposure of HL-60 cells to BT resulted in increased presence of reactive oxygen species (ROS), including superoxide ($O_2^{\bullet -}$), H_2O_2, HOCl, and hydroxyl radical (•OH), and consequent halogenative damage via the H_2O_2–MPO–HOCl system, which then induced apoptosis (Nishikawa et al., 2012). When the H_2O_2 resulting from BT exposure is metabolized to HOCl by MPO, the HOCl reacts with DNA or proteins to produce halogenated DNA or halogenated proteins. Since myeloid cells readily express MPO, and given that halogenated DNA may induce both genetic and epigenetic changes that contribute to carcinogenesis, our results may indicate how benzene is involved in bone marrow disorders or myeloid leukemia (Nishikawa et al., 2012).

In recent years, microarray analyses have been performed to elucidate gene-expression profile changes after exposure to benzene or its metabolites (Sarma et al., 2010; Sarma et al., 2011). No-one has yet published, however, profiles after exposure to BT. Moreover, because MPO is considered to play, as described above, a very important role in the carcinogenesis associated with benzene, we designed this study to clarify the toxicity of BT in human myeloid cell line HL-60 by obtaining gene expression profiles of HL-60 samples exposed to BT with or without MPO inhibition.

Materials and Methods

Reagents

BT was purchased from Wako Pure Chemical Industries, Ltd. (Osaka, Japan), and 4-aminobenzoic acid hydrazine (ABAH) was purchased from Tokyo Chemical Industry Co. Ltd. (Tokyo, Japan).

Cell culture

Human promyelocytic cell line HL-60 was kindly supplied by the Japanese Cancer Research Resource Bank (Osaka, Japan) and was cultured in RPMI 1640 medium (SIGMA-Aldrich, St. Louis, MO, USA) with 10% heat-inactivated fetal bovine serum (FBS) (Nichirei Biosciences Inc, Tokyo, Japan) at 37°C in a humidified 5% CO_2 incubator. To inactivate the complement, FBS was heated at 56°C for 30 min. Human lymphocytic cell line U937 was purchased from the European Collection of Cell Cultures (Salisbury, UK). It was cultured in the same way as HL-60.

BT exposure and ABAH treatment

HL-60 cells suspended at 4×10^5/mL density in RPMI 1640 with 10% of heat-inactivated FBS were incubated in 60 mm tissue culture dishes with and without BT (50 μM) at 37°C. For the MPO-inhibition experiment, HL-60 samples (4×10^5 cells/mL) were pretreated with 100 μM of ABAH in RPMI 1640 with 10% of heat-inactivated FBS at 37°C for 24 h. The suspension medium was then replaced with new medium containing the reagents (10% of heat-inactivated FBS and 100 μM of ABAH) plus BT (50 μM) and incubated at 37°C for 8 h. For control, unexposed HL-60 cells were suspended at 4×10^5/mL density in RPMI 1640 with 10% of heat-inactivated

FBS and incubated at 37°C in 60 mm tissue culture dishes. Samples of non-MPO-expressing U937 cells at 4×10^5/mL density were suspended in RPMI 1640 containing 10% of heat-inactivated FBS and incubated in 60 mm tissue culture dishes with or without BT (50 μM) at 37°C.

Measurement of apoptotic cells by flow cytometry

After HL-60 cells from standard cultures and samples cultured with ABAH were exposed to BT for 8 h, the cells were harvested and washed, and then stained, according to the manufacturer's instructions, with annexin V-fluorescein isothiocyanate (FITC) and propidium iodide (PI) double-labeling kits (TACS Annexin V-FITC Kit; Trevigen, Gaithersburg, MD, USA). Presence of apoptotic cells was evaluated using a FACScan flow cytometer (Becton, Dickinson, & Co., Mountain View, CA, USA), and data were analyzed using WinMDI software (ver. 2.9; Biology Software Net, La Habra, CA, USA). Apoptosis in U937 cell samples was evaluated using the same procedures.

Inhibition of MPO using by small interfering RNA

To inhibit the expression of *MPO*, RNA interference experiments were performed. Three *MPO* specific small interfering RNA (siRNA) were designed and synthesized according to manufacturer's instructions (OriGene Technologies, Inc. MD, USA). The three sequences used in this experiment were as follows: 5'-AGAAGCAUAUAGAGGCAAGAAAGAG-3'; 5'-ACUCCUAUCCUACUUCAAGCAGCCG-3'; and 5'-GCAACAUCAUCCGCAACCAGAU-3'. Samples of HL-60 cells at 7.1×10^4/mL

density suspended in RPMI-1640 with 10% FBS were transferred to 24-well plates and, according to the manufacturer‟s instructions, transfected with MPO-specific siRNA using OPTI-MEM® (Life Technologies Corp., CA, USA) at 37°C for 24 h. Samples from the wells were then harvested and washed with Dulbecco‟s phosphate-buffered saline (DPBS). These HL-60 cell pellets were then resuspended in 24-well plate at 40×10^4/mL density in RPMI-1640 with 10% FBS with and without 50 μM of BT at 40×10^4/mL and incubated for 8 h. After BT exposure, the presence of apoptotic cells was evaluated using flow cytometry as described above.

Detection of gene expression alteration induced by BT exposure

Total RNA isolation

According to manufacturers‟ instructions, total RNA was isolated from HL-60 cells using TRIzol Reagent (Invitrogen Corp., CA, USA) and purified using SV Total RNA Isolation System (Promega Corp., Madison, WI, USA). RNA samples were quantified using a NanoDrop ND-1000 spectrophotometer (Thermo Fisher Scientific Inc., Wilmington, DE, USA) and the quality of the RNA was checked using an Experion automated electrophoresis station (Bio-Rad Laboratories Inc., Hercules, CA, USA)

Gene expression microarrays

According to the manufacturer's instructions, the cRNA was amplified and labeled using Low Input Quick Amp Labeling (Agilent Technologies, Santa Clara, CA, USA), and hybridized using SurePrint G3 Human Gene Expression Microarray 8×60K v2

(Agilent). All hybridized microarray slides were scanned using an Agilent scanner. Relative hybridization intensities and background hybridization values were calculated using Agilent Feature Extraction Software (ver. 9.5.1.1).

Data analysis and filter criteria

Using procedures recommended by Agilent, raw signal intensities and flags for each probe were calculated from hybridization intensities (gProcessedSignal), and spot information (gIsSaturated, etc.). The raw signal intensities of samples (taken at 1 h and 4 h of Control vs. BT, Control vs. BT plus ABAH, BT vs. BT plus ABAH were $\log_2$-transformed and normalized using the quantile algorithm in the preprocessCore library package (Bolstad et al., 2003) in the Bioconductor application (Gentleman et al., 2004). We selected probes that registered P flags in at least one sample. To identify up- and down-regulated genes, we calculated intensity based Z-scores (Quackenbush, 2002) and ratios (non-log-scaled fold-change) from the normalized signal intensities of each probe and compared the controls (not exposed to BT) and experimental samples (with or without ABAH inhibition of MPO, exposed to BT). Then we established criteria for regulated genes: up-regulated genes, Z-score ≥ 2.0 and ratio ≥ 1.5-fold; down-regulated genes, Z-score ≤ -2.0 and ratio ≤ 0.66. To determine significantly over-represented GO categories and significant enrichment of pathways, we used tools and data provided at the *Database for Annotation, Visualization and Integrated Discovery* (DAVID) (http://david.abcc.ncifcrf.gov/home.jsp) (Huang et al., 2009). Results were generated from Control vs. BT and BT vs. BT plus ABAH. We generated a heat map using MeV

software (Saeed et al., 2003), and a hierarchical clustering (HCL) method to sort the genes. Color indicates the distance from the median of each row. The distance metric was "Pearson correlation", and the linkage method was "average linkage clustering".

Synthesis of cDNA and determination of gene expression by real-time PCR

After HL-60 cells were exposed to 50 μM BT as described above in „Measurement of apoptotic cells by flow cytometry" and total RNA was isolated from the cells as described in „Total RNA isolation", complementary DNA was synthesized by reverse transcription from total RNA using reverse transcriptase and oligo-dT20 (Toyobo Co. Ltd., Osaka, Japan). The resulting cDNA was amplified using SuperScript™ III (Invitrogen) under the following conditions: samples incubated at 95°C for 10 min, followed by 40 cycles alternating 60°C for 1 min and 95°C for 15 s. Real Time PCR was performed using a Thermal Cycler Dice® Real Time System (Takara Bio Inc., Otsu, Japan). The relative level of mRNA was calculated using cycle time (*Ct*) values, which were normalized against the value for glyceraldehyde-3-phosphate dehydrogenase (*GAPDH*). Using the $2^{-\Delta\Delta Ct}$ method (Livak et al., 2001), relative quantification (fold change) between different samples was calculated.

Statistical analysis

Data are shown as means + standard error (SE). Statistical analysis was performed using StatView version 5.0 for Windows (SAS, Institute Inc., Cary, NC, USA).

Differences between groups were tested by non-parametric Wilcoxon tests. A probability value of less than 0.05 was considered statistically significant. Fisher's exact test was used to detect statistically significantly over-represented GO categories and to characterize the enrichment of specific pathway components into functionally regulated gene groups.

Results

Proportions of apoptotic cells

Evaluation of apoptotic cells in HL-60 samples exposed to BT was performed using flow cytometry. More annexin V-positive and PI-negative cells, considered to be apoptotic, were detected in HL-60 samples that had been exposed to 50 μM BT for 8 h. Induction of apoptosis by BT in U937 samples was similarly evaluated. The percentage of apoptotic cells in HL-60 samples exposed to 50 μM BT was significantly greater than in unexposed samples (Fig. 1A). Furthermore apoptosis by BT was reduced by ABAH and siRNA targeting *MPO* (Fig. 1A, 1B). By contrast, no significant differences were found when comparing samples of U937 and MPO-negative cells that had or had not been exposed to 50 μM BT (Fig. 1C).

Identification of gene expression profiles in HL-60 cells exposed to BT

Whole genome microarray analysis of 50,599 gene expression changes was carried

out to identify the gene expression profiles of HL-60 cells after exposure to BT with or without MPO inhibition. Samples of HL-60 with or without ABAH were exposed to 50 μM BT for 1 h or 4 h. The data derived from this study have been deposited in the National Center for Biotechnology Information (NCBI) Gene Expression Omnibus (Edgar et al., 2002) and are accessible through the Gene Expression Omnibus (GEO) Series, Accession Number GSE50805 (http://www.ncbi.nlm.nih.gov/geo/query/acc.cgi?&acc=GSE50805).

After 1 h exposure to BT, statistically significant changes in the expression of 1,214 genes were apparent (751 up-regulated and 463 down-regulated). After 4 h exposure to BT, further statistically significant changes in the expression of 1,213 genes were apparent (817 up-regulated and 396 down-regulated). Table 1 lists the 20 genes most up- or down-regulated by 4 h exposure to BT. *MPO* ranked 9th among genes down-regulated after 4 h exposure to BT with ABAH. In HL-60 samples pretreated with ABAH to inhibit MPO, after 1 h exposure to BT, expression changes were detected in 225 genes (175 up-regulated and 50 down-regulated) and, after 4 h exposure, in 516 genes (406 up-regulated and 110 down-regulated). Expression changes in all of the 20 genes most up- or down-regulated by exposure to BT (Table 1) were less in samples pretreated with ABAH. To elucidate and visualize the differences in gene expression in normally cultured HL-60 cell samples exposed to BT and samples exposed to BT after pretreatment with ABAH, we carried out scatterplot analysis and clustering analysis (Figs. 2 and 3). Figure 2 shows scatterplots representing differences in gene expression amounts comparing BT and BT with ABAH. The gene expression HL-60 cell samples

exposed to BT increased relatively depending on length of exposure (blue circles in Fig. 2A and 2B). In samples in which MPO was inhibited by ABAH, however, the amount of gene expression was similar to HL-60 cell samples that had not been exposed to BT (red circles in Fig. 2A and 2B). Figure 3 shows gene expression patterns for samples exposed to 50 μM BT, specifically, heat maps for genes whose expression after exposure to BT with or without ABAH was statistically significantly different to control. In this study, statistically significantly altered expression was held to be $|\text{Z-score}| > 2.0$.

Pathway analysis

Genes with significantly different amounts of expression ($|\text{Z-score}| > 2.0$) across the various comparisons were imported into the DAVID v6.7 annotation tool, and GO and KEGG pathway analysis were carried out. Initial data were generated with 4 h BT-exposure group results and categorized based on GO terms with p-values < 0.05 (Table 2). Table 2 shows the ten most frequently derived GO functional categories thus obtained with data from samples exposed to BT for 4 h (upper rows) and pretreated with ABAH and then exposed to BT for 4 h (lower rows). While transcription, apoptosis, anti-apoptosis, proliferation, inflammation and cell-cycle-related genes were up-regulated by BT-exposure, cell-cycle-related genes were down-regulated when HL-60 cells were exposed to BT.

The enrichment of specific pathway components into functionally regulated gene groups was characterized with reference to the KEGG pathway

database. After exposure to BT for 4 h, the major genes identified were those involved in cytokine–cytokine receptor interaction, cancer, various signaling pathways including those involving chemokines, toll-like receptors, MAPK, NOD like receptors (NLR), cytosolic DNA-sensing, and p53 (Table 3). The upper rows in Table 3 show results for HL-60 cells exposed to BT, and the lower rows show results for HL-60 cells exposed to BT after pretreatment with ABAH. Figure 4 is a schematic diagram illustrating a signaling pathway that might result from BT exposure.

Validation of microarray findings with real-time PCR

To validate the microarray results, we selected the 20 genes that were found to have the most altered amount of gene expression in KEGG pathway analysis and performed real-time PCR for these 20 genes. *GAPDH* was used as an endogenous control in these protocols, and similar data were obtained from all samples. Real-time PCR data verified the results of microarray analysis (Table 4).

Discussion

To confirm the cytotoxicity of BT to HL-60 cells, we exposed samples to BT and measured percentages of apoptotic HL-60 cells in samples with or without MPO inhibition. Inhibiting MPO resulted in significantly lower counts of apoptotic cells (Fig. 1A and 1B). Additionally, we evaluated apoptosis, after exposure to BT, in samples of

human leukemic lymphoma cell U937, which does not express MPO. In U937 cell samples, BT had a negligible effect on apoptosis (Fig. 1C). Results obtained through these two different methods strongly suggest that the apoptosis induced by BT arises in the H_2O_2–MPO–HOCl system. While inhibition of MPO, at the protein stage with ABAH and at the transcription stage with siRNA, did reduce apoptosis caused by exposure to BT, the apoptotic cell counts were still higher than in control samples (Fig. 1A and 1B). This may indicate the presence of another pathway, not mediated by the H_2O_2–MPO–HOCl system, through which BT induces apoptosis. Or this discrepancy may indicate that there was insufficient inhibition of MPO by ABAH or siRNA.

In a previous study, we conjectured that exposing HL-60 cells to BT increases H_2O_2, which is then metabolized to HOCl by MPO; DNA and proteins are then halogenated by this HOCl, which thus may induce myelotoxicity or leukemogenesis. In other words, MPO plays a key role in benzene toxicity to myeloid cells. One way to clarify the role of MPO in benzene toxicity would be to examine the gene expression profiles of HL-60 cell samples in which MPO is inhibited just before BT exposure. Although MPO is considered to be a metabolic enzyme that helps to break down benzene (Schattenberg et al., 1994), it is also implicated in DNA and protein damage caused by BT toxicity, which ensues because the catalysis of MPO promotes the generation of HOCl, a powerful oxidant (Nishikawa et al., 2011). While gene expression profiles of myeloid cells exposed to benzene, hydroquinone (HQ), and benzoquinone (BQ) have been obtained (Sarma et al., 2011), no profiles of myeloid cells exposed to BT were available. Consequently, to clarify the relationships between myelotoxicity of benzene and MPO,

we analyzed the gene expression profiles of HL-60 human leukemia cells that were exposed to BT with or without MPO inhibition. Results showed, compared to 1 h exposure, an increase in up-regulated genes after 4 h and, conversely, a decrease in down-regulated genes. HL-60 cells exposed to BT with MPO-specific-inhibitor, ABAH, showed fewer gene changes than cells exposed to BT. We found negligible alteration in the amount of gene expression after exposure to ABAH (data not shown) and concluded that ABAH itself is unlikely to affect gene expression levels.

Profiles of HL-60 cells exposed to benzene, HQ, and BQ showed alterations in the expression profiles for genes related to cell proliferation, apoptosis, and cell death (Sarma et al., 2011). Similar profile changes were also found in HL-60 cells exposed to BT. In addition, we found marked changes in genes related to the cell cycle, inflammation, and antiapoptosis. These results suggest from the standpoint of cell survival, that BT toxicity is connected with the activation of *NF-κβ* and *cIAPs*, which induce antiapoptosis. Furthermore, there have been some recent reports that the *NF-κβ* signaling pathway is related to leukemogenesis (Nakagawa et al., 2011; Reikvam et al., 2009; Vilimas et al., 2007).

BT manifests cytotoxicity, including DNA damage, through the generation of ROS (Kawanishi et al., 1989; Kolanchana et al., 1993; Lewis et al., 1988), and the presence of ROS activates the mitogen-activated protein kinase (MAPK) signaling pathway (Gupta et al., 1999). Indeed, the results of our KEGG pathway analysis of HL-60 cells that had been exposed to BT showed significant up-regulation of *JUN*, *FOS*, *VEGF*, *MMPs* and *IL-8*, which are downstream of MAPK signaling pathway (Fig. 4). DNA

damage caused by ROS would activate the *p53* signaling pathway, which induces apoptosis. A cDNA microarray study of mouse bone marrow tissue that had been exposed to benzene suggests that the *p53* tumor suppressor gene, by strictly regulating specific genes involved in the pathways of cell cycle arrest, apoptosis, and DNA repair are a key mechanism in the harmful physical response to benzene (Yoon et al., 2003). Our current results also show marked up-regulation of cell-cycle-related genes (*GADD45A*, *SESN2*, *CDKN2B*, *PPM1D*) and apoptosis-related genes (*BAX* and *PUMA*) that are downstream of *p53*. Although it is known that HL-60 cells do not express *p53* (Wolf and Rotter., 1984), we discovered up-regulation of genes downstream from p53. This may indicate that HL-60 cells have another pathway, one which acts like a *p53* signaling pathway.

Conclusion

Table 5 lists the important findings from our study and promising paths for future investigation. Examining the gene expression of HL-60 cells exposed to BT with or without MPO inhibition, we found up-regulation of genes related to apoptosis, anti-apoptosis, proliferation, inflammation, and the cell cycle. This up-regulation was almost completely absent, however, when MPO-inhibited HL-60 samples were exposed to BT. The gene expression of HL-60 cells was altered dramatically simply by inhibiting MPO. These results indicate that MPO plays a crucial role in the cytotoxicity and leukemogenesis associated with benzene. In this study, we showed how HL-60 cells exposed to BT alter gene expression, and clarified the cytotoxic mechanism induced by

BT. It suggests that there may be a role for MPO as an examination marker or in prophylaxis for chemical carcinogenesis.

Legends

Fig. 1. Apoptosis. (For each figure, data from three independent experiments conducted in duplicate are presented as mean +SE). (A) Percentages of apoptotic HL-60 cells after 8 h exposure to BT with or without ABAH. (B) Percentages of apoptotic HL-60 cells after 8 h exposure to BT with or without MPO inhibition by siRNA. (C) Percentages of apoptotic U937 cells after 8 h exposure to BT with or without ABAH.

Fig. 2. Scatterplots representing the expression of genes in HL-60 cells exposed to 50 μM BT with or without ABAH for (A) 1 h or (B) 4 h. X-axis indicates the relative normalized $\log_2$-signal intensity of control (not exposed to BT) samples, and Y-axis indicates normalized $\log_2$-signal intensity of samples, with or without ABAH inhibition of MPO, exposed to BT. Blue dots in (A) and (B) denote BT-exposed samples and red dots show BT-exposed samples with ABAH pretreatment.

Fig. 3. Clustering diagram of gene trees and heatmap were generated by MeV software. We used a hierarchical clustering (HCL) method to sort the genes (The distance metric was “Pearson correlation”, and the linkage method was “average linkage clustering”). HL-60 cells were exposed to 50 μM BT for (A) 1 h or (B) 4 h with or without 100 μM ABAH. Rows represent the genes, and columns represent the samples. Colors indicate

the distance from the median of each row. Red blocks represent high, and green blocks low, expression relative to the control sample; black blocks indicate similar expression.

Fig. 4. Conjectural mechanism for BT cytotoxicity involved in myelotoxicity and leukemogenesis. Solid arrows indicate the activation of downstream genes and broken arrows show indirect effects.

References

Aksoy M., 1989. Hematotoxicity and carcinogenicity of benzene. Environ Health Perspect. 82: 193–197.

Bolstad B.M., Irizarry R.A., Astrand M., Speed T.P., 2003. A comparison of normalization methods for high density oligonucleotide array data based on variance and bias. Bioinformatics. 19: 185–193.

David W., Varda R., 1984. Major deletions in the gene encoding the p53 tumor antigen cause lack of p53 expression in HL-60 cells. Proc Natl Acad Sci USA. 82: 790–794.

Edgar, R., Domrachev, M., Lash, A.E., 2002. Gene Expression Omnibus: NCBI gene expression and hybridization array data repository. Nucleic Acids Res. 30: 207–210.

Gentleman R.C., Carey V.J., Bates D.M., Bolstad B., Dettling M., Dudoit S., Ellis B., Gautier L., Ge Y., Gentry J., Hornik K., Hothorn T., Huber W., Iacus S., Irizarry R., Leisch F., Li C., Maechler M., Rossini A.J., Sawitzki G., Smith C., Smyth G., Tierney L., Yang J.Y., Zhang J., 2004. Bioconductor: open software development for computational biology and bioinformatics. Genome Biol. 5: R80.

Gupta A., Rosenberger S.F., Bowden G.T., 1999. Increased ROS levels contribute to elevated transcription factor and MAP kinase activities in malignantly progressed mouse keratinocyte cell lines. Carcinogenesis. 20: 2063–2073.

Harrison J.E., Schultz J., 1976. Studies on the chlorinating activity of myeloperoxidase. J Biol Chem. 251: 1371–1374.

Heller J.I., Crowley J.R., Hazen S.L., Salvay D.M., Wagner P., Pennathur S., et al., 2000. *p-Hydroxyphenylacetaldehyde,* an aldehyde generated by myeloperoxidase, modifies phospholipid amino groups of low density lipoprotein in human atherosclerotic intima. J Biol Chem. 275: 9957–9962.

Huang DW, Sherman BT, Lempicki RA., 2009. Systematic and integrative analysis of large gene lists using DAVID Bioinformatics Resources. Nature Protoc. 4: 44-57.

Huang DW, Sherman BT, Lempicki RA., 2009. Bioinformatics enrichment tools: paths toward the comprehensive functional analysis of large gene lists. Nucleic Acids Res. 37: 1-13.

Huff J., 2007. Benzene-induced cancers: abridged history and occupational health impact. Int J Occup Environ Health. 13: 213–221.

Hurst J.K., Barrette W.C. Jr., 1989. Leukocytic oxygen activation and microbicidal oxidative toxins. Crit Rev Biochem Mol Biol. 24: 271–328.

Kawanishi S., Inoue S., Kawanishi M., 1989. Human DNA damage induced by 1, 2, 4-benzenetriol, a benzene metabolite. Cancer Res. 49: 164–168.

Klebanoff S.J., 1999. Myeloperoxidase. Proc Assoc Am Physicians. 111: 383–389.

Kolachana P., Subrahmanyam V.V., Meyer K.B., Zhang L., Smith M.T., 1993. Benzene and its phenolic metabolites produce oxidative DNA damage in HL60 cells in vitro and in the bone marrow in vivo. Cancer Res. 53: 1023–1026.

Kanehisa M., Goto S., 2000. KEGG: Kyoto Encyclopedia of Genes and Genomes. Nucleic Acids Res. 28: 27–30.

Lewis J.G., Stewart W., Adams D.O., 1988. Role of oxygen radicals in induction of DNA damage by metabolites of benzene. Cancer Res. 48: 4762–4765.

Livak K.J., Schmittgen T.D., 2001. Analysis of relative gene expression data using real-time-quantitative PCR and the $2^{-\Delta\Delta Ct}$ method. Methods. 25: 402–408.

Marnett L.J., 2000. Oxyradicals and DNA damage. Carcinogenesis. 21: 361–370.

Nakagawa M., Shimabe M., Watanabe-Okochi N., Arai S., Yoshimi A., Shinohara A., Nishimoto N., Kataoka K., Sato T., Kumano K., Nannya Y., Ichikawa M., and Kurokawa M., 2011. AML1/RUNX1 functions as a cytoplasmic attenuator of NF-κB signaling in the repression of myeloid tumors. Blood. 118: 6626–6637.

Nishikawa T., Miyahara E., Horiuchi M., Izumo K., Okamoto Y., Kawai Y., Kawano Y., and Takeuchi T., 2012. Benzene metabolite 1, 2, 4-Benzenetriol induces halogenated DNA and tyrosine representing halogenative stress in the HL-60 human myeloid cell line. Environmental Health Perspect. 120: 62–67.

Nishikawa T., Izumo K., Miyahara E., Horiuchi M., Okamoto Y., Kawano Y., and Takeuchi T., 2011. Benzene induces cytotoxicity without metabolic activation. J Occup Health. 53: 84–92.

Quackenbush J., 2002. Microarray data normalization and transformation. Nat Genet. 32: 496–501.

Reikvam H., Olsnes A.M., Gjertsen BT., Ersvar E., Bruserud Ø., 2009. Nuclear factor-kappaB signaling: a contributor in leukemogenesis and a target for pharmacological intervention in human acute myelogenous leukemia. Crit Rev Oncog. 15: 1–41.

Saeed A.I., Sharov V., White J., Li J., Liang W., Bhagabati N., Braisted J., Klapa M., Currier T., Thiagarajan M., Sturn A., Snuffin M., Rezantsev A., Popov D., Ryltsov A., Kostukovich E., Borisovsky I., Liu Z., Vinsavich A., Trush V., Quackenbush J., 2003. TM4: a free, open-source system for microarray data management and analysis. Biotechniques. 34: 374–378.

Sailendra N.S., Kim Y.J., Ryu J.C., 2010. Gene expression profiles of human promyelocytic leukemia cell lines exposed to volatile organic compounds. Toxicology. 271: 122–130.

Sailendra N.S., Kim Y.J., Ryu J.C., 2011. Differential gene expression profiles of human leukemia cell lines exposed to benzene and its metabolites. Environmental Toxicology and Pharmacology. 32: 285–295.

Schattenberg D.G., Stillman W.S., Gruntmeir J.J., Helm K.M., Irons R.D., Ross D., 1994. Peroxidase activity in murine and human hematopoietic progenitor cells: potential relevance to benzene-induced toxicity. Mol Pharmacol. 46: 346–51.

Snyder R., Hedli C.C., 1996. An overview of benzene metabolism. Environ Health Perspect. 104: 1165–1171.

Vilimas T., Mascarenhas J., Palomero T., Mandal M., Buonamici S., Meng F., Thompson B., Spaulding C., Macaroun S., Alegre ML., Kee BL., Ferrando A., Miele L., Aifantis I., 2007. Targeting the NF-kappaB signaling pathway in Notch1-induced T-cell leukemia. Nat Med. 13: 70–77.

Ward J.F., Limoli C.L., Calabro-Jones P., Evans J.W., 1987. Radiation versus chemical damage to DNA. In Cerutti P.A., Nygaard O.F. and Simic M.G. (eds) Anticarcinogenesis and Radiation Protection. Plenum, New York. 321–327.

Yoon B.I., Li G.X., Kitada K., Kawasaki Y., Igarashi K., Kodama Y., Inoue T., Kobayashi K., Kanno J., Kim D.Y., Inoue T., Hirabayashi Y., 2003. Mechanisms of benzene-induced hematotoxicity and leukemogenicity: cDNA microarray analyses using mouse bone marrow tissue. Environ Health Perspect. 111: 1411–20.

Table 1. HL-60 cells after 4 h exposure to BT: 20 most up- and down-regulated genes from the total 50,599 genes

Gene Symbol	Acc#	Z score	Gene name
HMOX1	NM_002133	12.72	heme oxygenase (decycling) 1
TNFAIP6	NM_007115	11.03	tumor necrosis factor, alpha-induced protein 6
JUN	NM_002228	9.108	jun proto-oncogene
CCL4	NM_002984	9.071	chemokine (C-C motif) ligand 4
IL8	NM_000584	8.548	interleukin 8
KLHDC7B	NM_138433	8.388	kelch domain containing 7B
ATF3	NM_001040619	8.136	activating transcription factor 3
RELB	NM_006509	7.802	v-rel avian reticuloendotheliosis viral oncogene homolog B
BCL3	NM_005178	7.511	B-cell CLL/lymphoma 3
CXCL2	NM_002089	7.384	chemokine (C-X-C motif) ligand 2
EGR1	NM_001964	7.235	early growth response 1
DDIT4	NM_019058	7.141	DNA-damage-inducible transcript 4
CXCL3	NM_002090	6.925	chemokine (C-X-C motif) ligand 3
NFKBIA	NM_020529	6.842	nuclear factor of kappa light polypeptide gene enhancer in B-cells inhibitor, alpha
BIRC3	NM_001165	6.795	baculoviral IAP repeat containing 3
CHAC1	NM_024111	6.771	ChaC, cation transport regulator homolog 1
SESN2	NM_031459	6.750	sestrin 2
KLF2	NM_016270	6.636	Kruppel-like factor 2 (lung)
KLHDC7B	NM_138433	6.546	kelch domain containing 7B
LOC344887	NR_033752	6.415	NmrA-like family domain containing 1 pseudogene
Gene Symbol	Acc#	Z score	Gene name
XLOC_005827	BE387254	–6.768	cDNA clone IMAGE:3616431
PRTN3	NM_002777	–4.871	proteinase 3
RILP	NM_031430	–4.785	Rab interacting lysosomal protein
RTN4R	NM_023004	–4.744	reticulon 4 receptor
TTTY13	NR_001537	–4.231	testis-specific transcript, Y-linked 13 (non-protein coding)
DGAT2	NM_032564	–4.221	diacylglycerol O-acyltransferase 2
TLR9	NM_017442	–3.742	toll-like receptor 9
PTPN3	NM_002829	–3.721	protein tyrosine phosphatase, non-receptor type 3
CD3EAP	NM_012099	–3.710	CD3e molecule, epsilon associated protein
TNFRSF8	NM_001243	–3.588	tumor necrosis factor receptor superfamily, member 8
ANKRD19P	AK292218	–3.582	cDNA FLJ77364 complete cds, highly similar to ankyrin repeat domain 19
PRDM12	NM_021619	–3.503	PR domain containing 12
ZBTB42	NM_001137601	–3.322	zinc finger and BTB domain containing 42
LINGO3	NM_001101391	–3.314	leucine rich repeat and Ig domain containing 3
STEAP3	NM_182915	–3.271	STEAP family member 3, metalloreductase
NANOS1	NM_199461	–3.259	nanos homolog 1
ENG	NM_000118	–3.246	endoglin
C17orf87	NM_207103	–3.243	SLP adaptor and CSK interacting membrane protein
NANP	NM_152667	–3.240	N-acetylneuraminic acid phosphatase
PDE11A	NM_001077358	–3.217	phosphodiesterase 11A

Table 2. GO functional category analysis of genes differentially expressed in HL-60 cells in response to BT for 4 h and HL-60 cells similarly exposed to BT after pretreatment with ABAH.

Term	Count	*p*-value
Regulation of transcription	109	2.8×10^{-7}
Transcription	81	3.3×10^{-4}
Regulation of RNA metabolic process	72	3.5×10^{-4}
Regulation of Transcription, DNA-dependent	71	3.1×10^{-4}
Intracellular signaling cascade	57	6.4×10^{-5}
Regulation of apoptosis	51	1.2×10^{-8}
Regulation of programmed cell death	51	1.7×10^{-8}
Regulation of cell death	51	1.8×10^{-8}
Immune response	47	5.9×10^{-9}
Regulation of cell proliferation	46	7.6×10^{-7}
Term	Count	*p*-value
Regulation of transcription	73	7.1×10^{-6}
Transcription	54	1.6×10^{-3}
Regulation of RNA metabolic process	49	1.0×10^{-3}
Regulation of transcription, DNA-dependent	47	2.0×10^{-3}
Immune response	39	1.1×10^{-10}
Regulation of apoptosis	37	8.4×10^{-8}
Regulation of programmed cell death	37	1.1×10^{-7}
Regulation of cell death	37	1.2×10^{-7}
Positive regulation of cellular biosynthetic process	32	5.9×10^{-7}
Positive regulation of biosynthetic process	32	8.1×10^{-7}

DAVID v6.7 functional annotation bioinformatics microarray analysis software was used to obtain the GO biological process functional category. Only GO terms for categories that showed statistically significantly differences in the amount of genes (compared with control) are shown (*p*-value $\leq$ 0.05).

Table 3. KEGG pathway functional classification of genes in HL-60 cells differentially expressed after exposure to BT for 4 h and HL-60 cells similarly exposed to BT after pretreatment with ABAH .

Term	Count
Cytokine–cytokine receptor interaction	22
Chemokine signaling pathway	18
MAPK signaling pathway	16
NOD-like receptor signaling pathway	12
Toll-like receptor signaling pathway	12
Systemic lupus erythematosus	9
RIG-I-like receptor signaling pathway	8
p53 signaling pathway	7
Epithelial cell signaling in *Helicobactor pylori* infection	7
B cell receptor signaling pathway	7
Term	Count
Cytokine–cytokine receptor interaction	18
Chemokine signaling pathway	16
Pathways in cancer	12
Toll-like receptor signaling pathway	11
MAPK signaling pathway	11
NOD-like receptor signaling pathway	10
Cytosolic DNA-sensing pathway	6
Systemic lupus erythematosus	6
Epithelial cell signaling in *Helicobactor pylori* infection	5
p53 signaling pathway	5

DAVID v6.7 functional annotation bioinformatics microarray analysis software was used to obtain the KEGG pathway functional classification. Only KEGG pathway terms for classification that showed statistically significantly differences in the amount of genes (compared with control) are shown (p-value $\leq$ 0.05).

Table 4. Expression of genes, detected by real-time PCR, associated with HL-60 cell exposure to BT

Gene symbol	Fold changes	
	Control vs. BT	Control vs. ABAH+BT
Apoptosis		
GADD45A	7.52 (+ 0.0638)	2.48 (+0.0289)
DDIT3	25.3 (+ 0.112)	6.53 (+0.0774)
DUSP1	45.7 (+ 0.0867)	5.88 (+0.0689)
NFKBIA	61.8 (+ 0.0838)	7.47 (+0.0396)
Carcinogenesis		
BBC3	16.5 (+0.551)	4.64 (+0.476)
FOS	14.9 (+ 0.156)	2.17 (+0.140)
JUN	52.5 (+ 0.409)	4.13 (+0.307)
MMP9	12.3 (+0.0978)	2.11 (+0.0448)
PPM1D	4.19 (+ 0.234)	1.02 (+0.331)
SESN2	78.1 (+ 0.504)	8.94 (+0.483)
VFGFA	9.62 (+ 0.305)	2.07 (+0.340)
Regulation of transcription		
RELB	34.7 (+ 0.572)	7.41 (+0.554)
CREBBP	3.12 (+ 0.466)	1.19 (+0.539)
Cell cycle regulation		
CDKN1C	3.30 (+ 0.0350)	0.950 (+0.0225)
CDKN2B	6.98 (+ 0.215)	2.31 (+0.531)
Immune responses		
IL1B	8.07 (+ 0.0675)	2.13 (+0.0603)
IL8	215 (+0.0975)	41.7 (+0.0712)
NFKB2	42.2 (+0.414)	5.28 (+0.477)
Oxidative stress		
HSP6A	46.5 (+ 0.247)	4.72 (+0.266)
Others		
MPO	0.556 (+ 0.143)	0.439 (+0.261)

Table 5. Important findings and implications of this study.

Important findings
・With MPO inhibition, BT hardly increased apoptosis in HL-60 cells. ・BT did not increase apoptosis in U937 cells, which express no MPO. ・Apoptosis, antiapoptosis, proliferation, inflammation and cell-cycle-related genes were up-regulated by BT exposure. When MPO was inhibited, however, the up-regulation was reduced: simple inhibition dramatically altered the gene expression of HL-60 cells.
Implications
・MPO may become a promising target molecule to prevent development of AML or bone marrow suppression via ROS generation. ・Measurement of MPO activity may be used as a biomarker to assess the risk of AML or bone marrow suppression for people who are occupationally exposed to benzene. ・MPO inhibitors, such as ABAH, may be helpful in preventive or therapeutic medicine.

Figure 1.

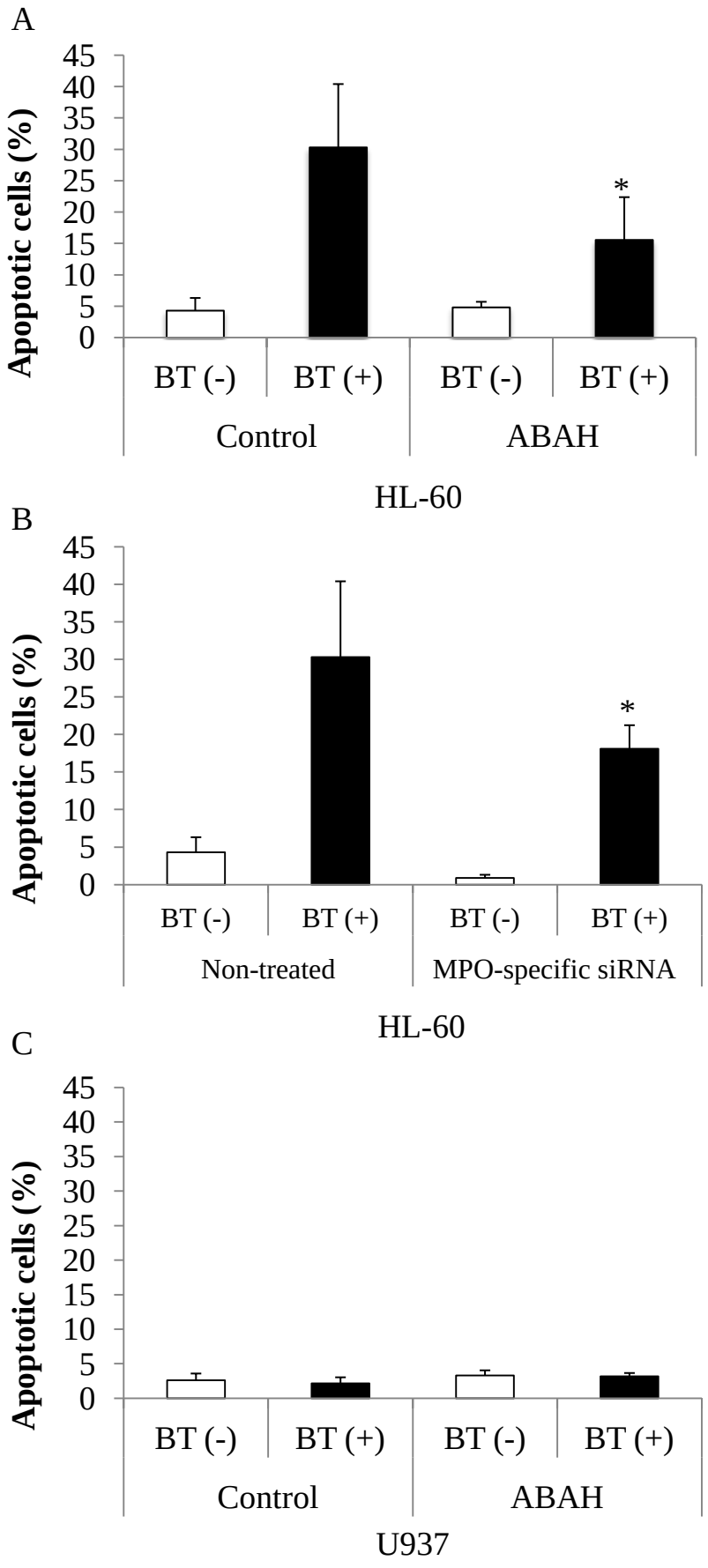
A
Apoptotic cells (%)
45
40
35
30
25
20
15
10
5
0
*
BT (-)
BT (+)
BT (-)
BT (+)
Control
ABAH
HL-60
B
Apoptotic cells (%)
45
40
35
30
25
20
15
10
5
0
*
BT (-)
BT (+)
BT (-)
BT (+)
Non-treated
MPO-specific siRNA
HL-60
C
Apoptotic cells (%)
45
40
35
30
25
20
15
10
5
0
BT (-)
BT (+)
BT (-)
BT (+)
Control
ABAH
U937

Figure 2.

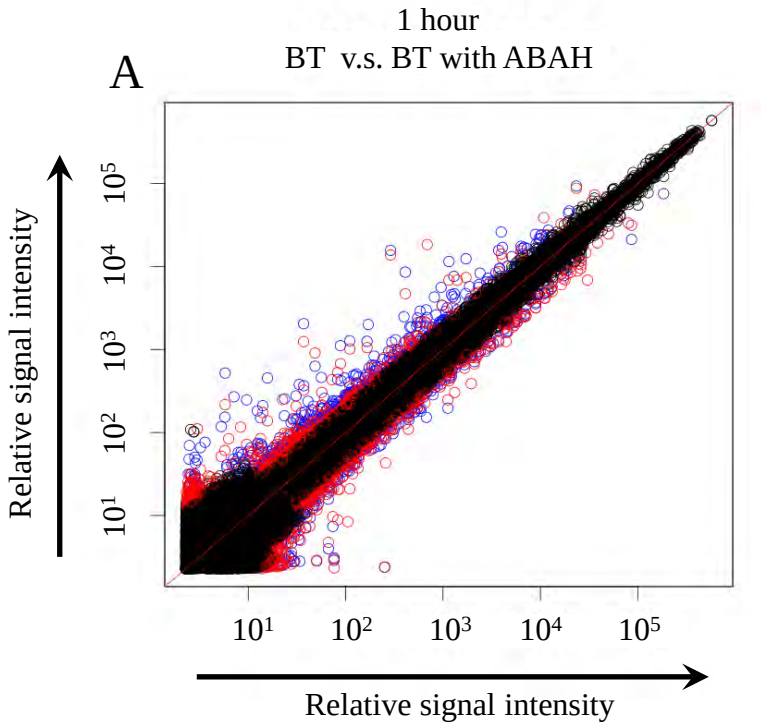
1 hour
BT v.s. BT with ABAH
A
Relative signal intensity
10^1
10^2
10^3
10^4
10^5
Relative signal intensity

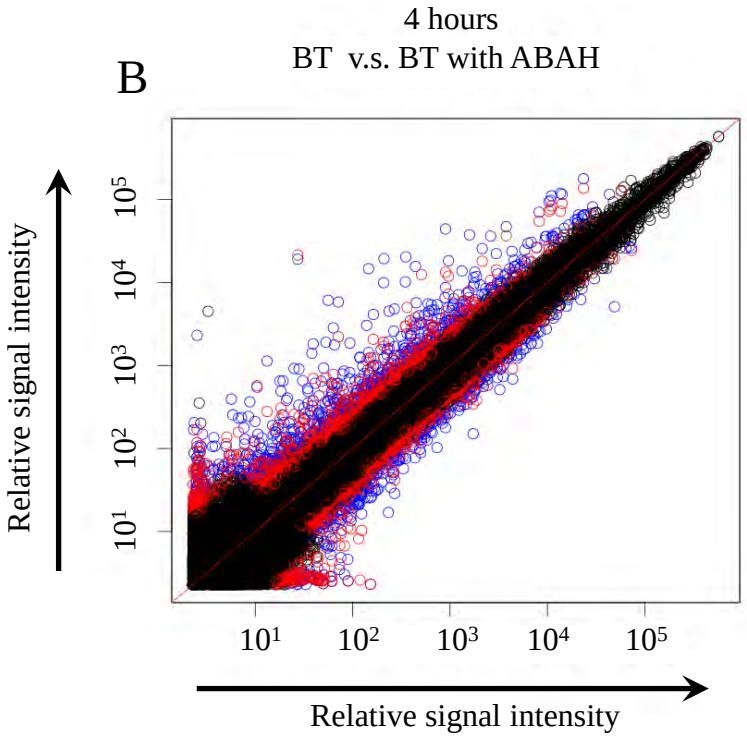
4 hours
BT v.s. BT with ABAH
B
Relative signal intensity
10^1
10^2
10^3
10^4
10^5
Relative signal intensity

Figure 3.

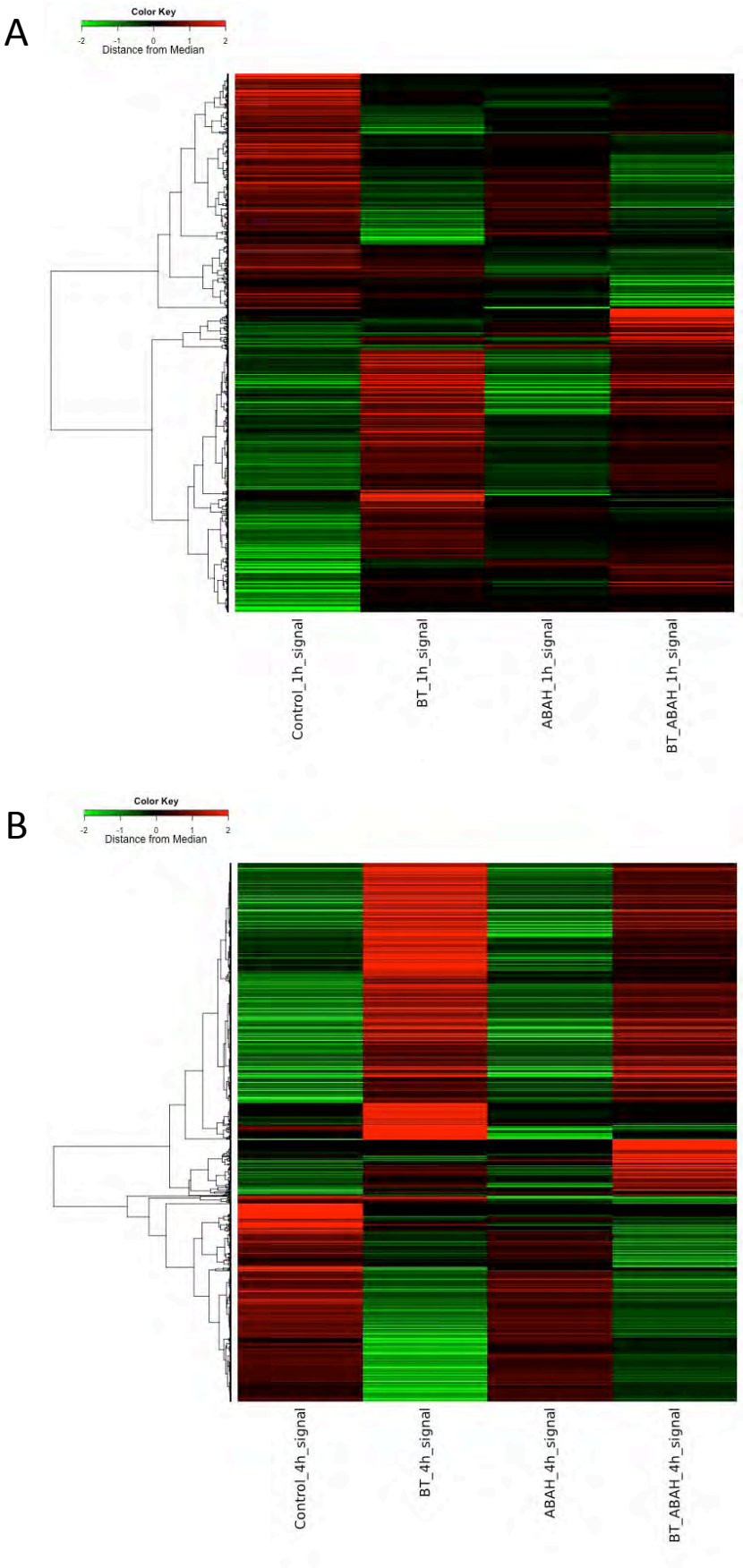
A
Color Key
-2 -1 0 1 2
Distance from Median
Control_1h_signal
BT_1h_signal
ABAH_1h_signal
BT_ABAH_1h_signal
B
Color Key
-2 -1 0 1 2
Distance from Median
Control_4h_signal
BT_4h_signal
ABAH_4h_signal
BT_ABAH_4h_signal

Figure 4.

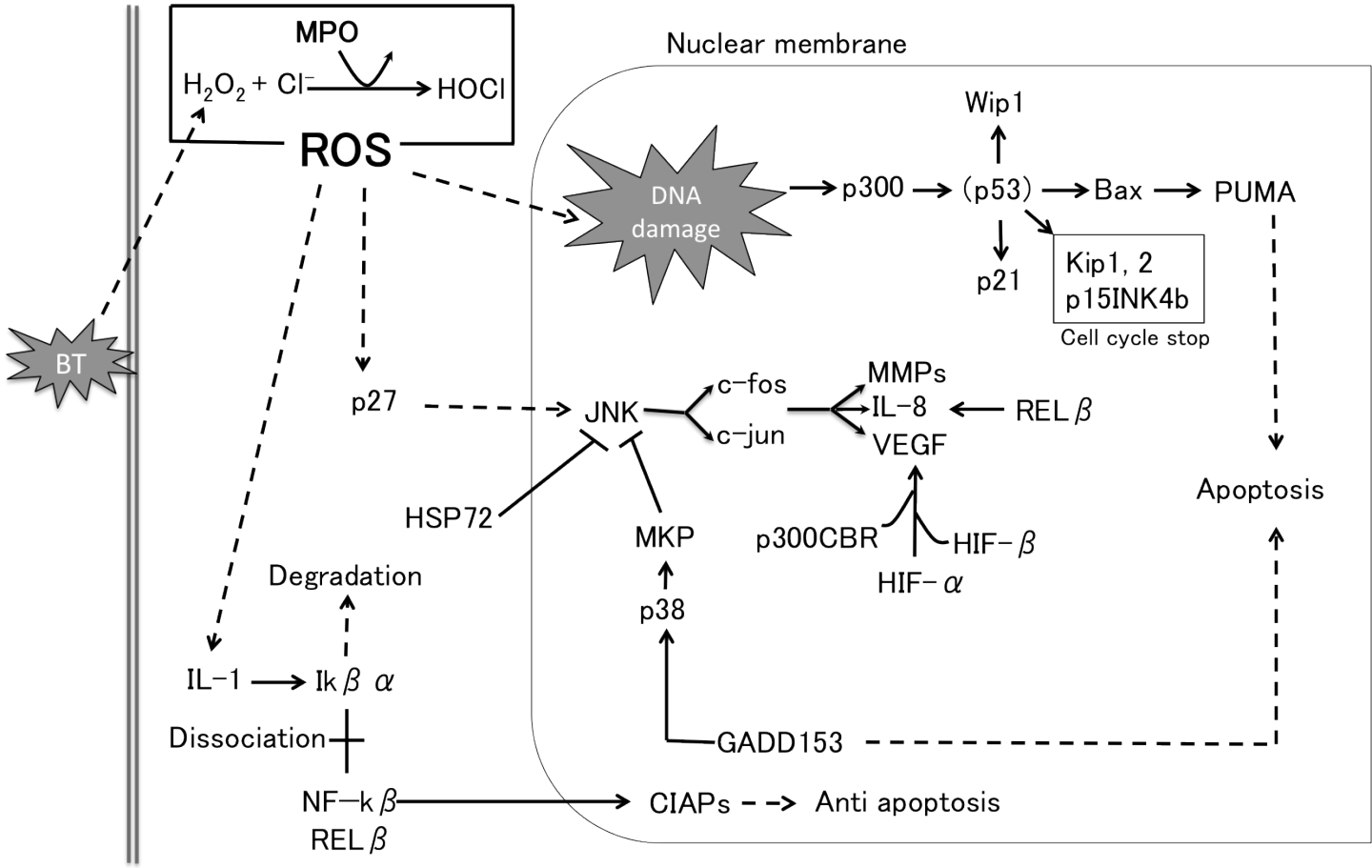
MPO
$H_2O_2 + Cl^-$
HOCl
ROS
Nuclear membrane
DNA damage
p300
(p53)
Wip1
Bax
PUMA
p21
Kip1, 2
p15INK4b
Cell cycle stop
BT
p27
JNK
c-fos
c-jun
MMPs
IL-8
VEGF
REL β
HSP72
MKP
p300CBR
HIF-β
HIF-α
Apoptosis
Degradation
IL-1
Ik β α
Dissociation
p38
GADD153
NF-k β
REL β
CIAPs
Anti apoptosis